

Supramolecular interactions in clusters of polar and polarizable molecules

Francesca Terenziani and Anna Painelli*

Dip. di Chimica GIAF Università di Parma, I-43100 Parma, Italy; INSTM-UdR Parma

(Dated: January 14, 2022)

We present a model for molecular materials made up of polar and polarizable molecular units. A simple two state model is adopted for each molecular site and only classical intermolecular interactions are accounted for, neglecting any intermolecular overlap. The complex and interesting physics driven by interactions among polar and polarizable molecules becomes fairly transparent in the adopted model. Collective effects are recognized in the large variation of the molecular polarity with supramolecular interactions, and cooperative behavior shows up with the appearance, in attractive lattices, of discontinuous charge crossovers. The mf approximation proves fairly accurate in the description of the gs properties of MM, including static linear and non-linear optical susceptibilities, apart from the region in the close proximity of the discontinuous charge crossover. Sizeable deviations from the excitonic description are recognized both in the excitation spectrum and in linear and non-linear optical responses. New and interesting phenomena are recognized near the discontinuous charge crossover for non-centrosymmetric clusters, where the primary photoexcitation event corresponds to a multielectron transfer.

PACS numbers: 78.20.Bh, 78.40.Me, 71.35.-y, 42.65.An

I. INTRODUCTION

The promise of molecular materials (MM) for advanced applications is impressive: not only *old* devices can be fabricated by light-weighted, flexible and cheap materials, but a new generation of devices is likely to appear to drive a molecular electronic and/or photonic revolution. Large non-linear responses to external perturbations (including electrical and optical fields) are required for applications and functional MM are often based on π -conjugated molecules and polymers. Structure-properties relationships are well understood at the molecular level at least for a few families of molecules,^{1,2} and the guided synthesis of molecules with specified behavior has already been demonstrated.^{3,4} But as the synthetic ability evolves from the molecular to the supramolecular level,⁵ interpretative tools are required to guide the synthesis at all stages, and supramolecular structure-properties relationships must be devised.

Extending our comprehension of the properties of MM from the molecular to the supramolecular level is a challenging task since non-additive, collective behavior appears in MM as a results of intermolecular interactions. Particularly important collective effects are expected in functional MM based on large (and largely polarizable) π -conjugated molecules, as it was suggested by McConnell, 40 years ago,⁶ and as it was more recently underlined with specific reference to MM for non-linear optical (NLO) applications.⁷

The mean-field (mf) approach is a simple approximation scheme to describe the ground state (gs) of MM. Within mf the problem of N interacting molecules factorizes into N effective molecular problems and collectivity is introduced by the local self-consistent fields generated by the surrounding at each molecular site. Recently the mf approximation was implemented into a quantum

chemical calculation of the polarization of crystals and films of large conjugated molecules.^{8,9,10} The charge distribution on polarizable molecular sites is strongly affected by local electric fields, and prominent collective behavior is recognized in the very large on-site charge redistribution in crystals of quadrupolar molecules.^{8,9} So far the approach was not applied to crystals or films of polar molecules, where even larger effects are expected.

The mf approximation does not apply to excited states, that in MM are usually described within the excitonic approach, a very popular approximation scheme originally developed for weakly interacting MM.^{11,12} In this limit sizeable collective phenomena are expected only if intermolecular interactions mix up degenerate (or quasi-degenerate) states. Within the excitonic model, then, any interaction among states with a different number of excitations is disregarded. The mf approximation supports collective behavior, but suppresses any correlation of the electronic motion on different molecules. The excitonic approximation instead describes *collective and correlated* excited states.¹³ But, not accounting for the mixing of states with a different number of excitations, the excitonic model disregards the molecular polarizability, a serious limitation for MM of interest for advanced applications. Moreover, the excitonic model relies on the definition of molecular (local) ground and excited states, as states relevant to the molecule embedded in the material, but no hint is given on how to derive these effective states from the molecular and supramolecular structure.^{11,12,13}

In clusters of non-polar molecules leading supramolecular interactions are represented by electrostatic interactions between transition dipole moments: the resulting J -term in the excitonic model describes exciton hopping between different sites.¹² The same interaction is also responsible for the so-called non-Heitler-London term:¹² this term, neglected in the excitonic approxima-

tion, mixes up states whose exciton number differs by two units. A recent detailed study has demonstrated that this term has indeed only minor effects in aggregates of non-polar chromophores.¹⁴

The simple excitonic model derived for materials made up of non-polar molecules is often adopted, with no further scrutiny, to describe materials based on polar molecules. In this case, however, additional interactions appear due to the finite permanent dipole moments of the molecular units in both the ground and excited states. In particular, the interaction between permanent dipole moments on different molecular units introduces in the Hamiltonian an exciton-exciton interaction term. This term conserves the exciton number and therefore survives in the excitonic approximation. The role of the exciton-exciton interaction in promoting bound-exciton states (and specifically biexcitons) in layers of polar molecules, was investigated in ref. 15. The formation of exciton strings was also discussed in ref. 17 as a consequence of exciton-exciton interactions in models for linear aggregates. This same concept was applied in a different context, to explain anomalous spectral features in differential transmission spectra of organic charge-transfer (CT) salts with a mixed donor-acceptor (D-A) stack motif,^{18,19} leading to the experimental confirmation of bound exciton states.

The excitonic model was developed to describe MM in the limit of weak interactions, i.e. for intermolecular energies much smaller than intramolecular excitation energies.^{11,12} Electrostatic interactions among polar molecules are instead large, and can easily be of similar magnitude or even larger than the small excitation energies typical of largely polarizable molecules. The failure of the excitonic model to describe interacting polar and polarizable molecules is therefore hardly surprising. However, since current understanding of optical properties of MM generally relies on the excitonic picture, it is important to explicitly discuss the limits of this approximation. We will show that the properties of MM based on polar and polarizable molecules are quantitatively as well as qualitatively different from the sum of the molecular properties. New and interesting physics appears in these materials due to supramolecular interactions, and it cannot be appreciated within standard approximation schemes.

In this paper we discuss the gs and the excitation spectrum of a simple model for clusters of polar and polarizable chromophores. Each molecular unit is described in terms of the Mulliken model.²⁰ This two state model was originally proposed to describe D-A CT complexes in solution.²⁰ Later it was adopted to model NLO responses of push-pull chromophores,²¹ an interesting class of π -conjugated molecules with electron D and A end groups. In this context the Mulliken model, extended to account for the interaction with internal vibrations and/or with solvation degrees of freedom, offered an accurate description of low-energy spectral properties of solvated push-pull chromophores.^{22,23} Intermolecular interactions are

introduced in terms of classical electrostatic forces, any intermolecular charge resonance being disregarded (zero intermolecular overlap approximation).⁸ The resulting model quite naturally applies to MM based on push-pull chromophores. By choosing different geometries for the cluster, the model describes different kinds of materials, like, e.g., aggregates, Langmuir-Blodgett (LB) films, functionalized polymers, and molecular crystals.

In a different context, one-dimensional (1D) models for aligned polar and polarizable units, only interacting via electrostatic forces offered a first description of the neutral-ionic (N-I) phase transition observed in CT crystals with a mixed stack motif.²⁴ This model is fairly crude, since it reduces a stack of overlapping molecules (...D-A-D-A....) to a collection of non-overlapping dimers (...D-A D-A....). In spite of that, a mf description of the relevant gs offered a first picture for the N-I transition, and specifically for the crossover from a continuous N-I interface to a discontinuous transition at large electrostatic interactions.²⁴ More recently the same model, within the excitonic approximation, yielded an interesting picture for the excitation spectrum of mixed stack CT salts with a largely N gs.^{18,19}

II. THE MODEL

The Mulliken model²⁰ was originally proposed to describe charge resonance in isolated D-A complexes on the basis of the two limiting neutral (N) and ionic (I) states: $|DA\rangle$ and $|D^+A^-\rangle$, respectively. The same model describes intramolecular charge resonance in push-pull chromophores where the same two basis states describe the limiting apolar and charge-separated (zwitterionic) structure,²¹ as schematically shown in Fig. 1 for a typical chromophore. Following Mulliken, we disregard all matrix elements of the dipole moment operator, except the dipole moment of the charge separated, ionic (I) state, $\langle D^+A^-|\hat{\mu}|D^+A^-\rangle = ea$, where a measures the distance between D and A molecules in CT complexes or an effective molecular length in push-pull chromophores. If $2z_0$ is the energy gap between the two basis states, and $-\sqrt{2}t$ is the mixing matrix element (in the following we will fix $\sqrt{2}t$ as the energy unit), the Mulliken Hamiltonian is written as:

$$H = 2z_0\hat{\rho} - \sqrt{2}t\hat{\sigma}_x \quad (1)$$

where $\hat{\rho} = \hat{\sigma}_z + 1/2$ is the ionicity operator, measuring the degree of CT from D to A , and $\hat{\sigma}_{x/z}$ are the Pauli matrices.

The solution of this Hamiltonian is trivial. The resulting ground and excited state are linear combinations of the two basis states, and the amount of mixing is defined in terms of a single parameter:

$$\rho = \frac{1}{2} - \frac{z_0}{2\sqrt{z_0^2 + 1}}, \quad (2)$$

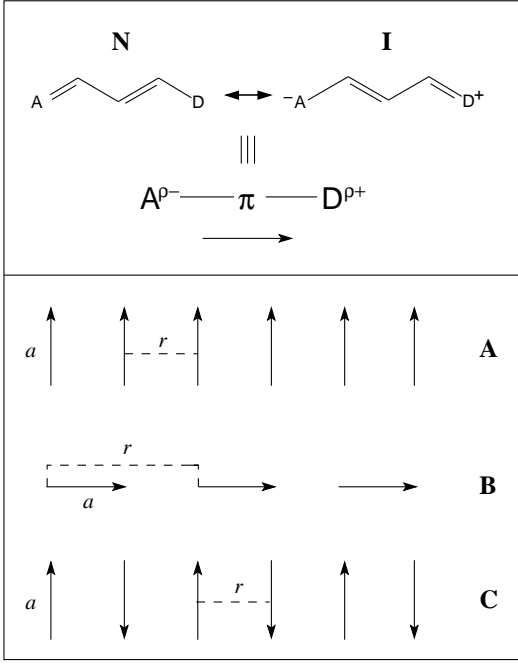


FIG. 1: Upper panel: schematic representation of a push-pull chromophores in terms of the two limiting neutral (N) and charge-separated, ionic (I) forms. The average charge separation in the ground state, ρ , is proportional to the molecular dipole moment, shown in the figure as an arrow. Lower panel: the three one-dimensional lattices considered in this paper. Each molecule is represented by an arrow, showing its ground-state dipole moment.

as follows:

$$\begin{aligned} |G\rangle &= \sqrt{1-\rho}|DA\rangle + \sqrt{\rho}|D^+A^-\rangle \\ |E\rangle &= \sqrt{\rho}|DA\rangle - \sqrt{1-\rho}|D^+A^-\rangle \end{aligned} \quad (3)$$

ρ is the gs expectation value of the charge operator and is proportional to the gs molecular dipole moment: $\langle G|\hat{\mu}|G\rangle = e a \rho$.

We describe a MM made up of polar and polarizable molecules as a collection of Mulliken-molecules (i.e. of molecules described by the Hamiltonian in Eq. (1)) interacting via classical electrostatic forces. The relevant Hamiltonian reads:

$$H = \sum_i \left(2z_0 \hat{\rho}_i - \sqrt{2} t \hat{\sigma}_{x,i} \right) + \sum_{i>j} V_{ij} \hat{\rho}_i \hat{\rho}_j \quad (4)$$

where i, j count the molecular sites, and the index on $\hat{\rho}$ and $\hat{\sigma}_x$ specifies them as operators working on the corresponding site. V_{ij} measures the electrostatic interaction between two fully-I molecules on sites i and j . Different choices are possible for V_{ij} : dipolar interactions are unrealistic for typical push-pull chromophores whose length (~ 10 Å) is similar to the intermolecular distances. We

therefore model each molecule in the I ($|D^+A^-\rangle$) state as a segment of length a bearing $+/-$ charges at the D/A ends, and then calculate V_{ij} based on unscreened Coulomb interactions. Specifically, for the three 1D lattices sketched in Fig. 1 we have:

$$V_{ij} = (\pm 1)^{i-j} 2vw \left[\frac{1}{d_{ij}} - \frac{1}{\sqrt{d_{ij}^2 + w^2}} \right] \quad (5)$$

where the $+/-$ sign refers to A/C lattices, and

$$V_{ij} = 2vw \left[\frac{1}{d_{ij}} - \frac{d_{ij}}{d_{ij}^2 - w^2} \right] \quad (6)$$

for B lattices. In all cases d_{ij} is the distance between sites i and j , in units of the distance r between adjacent sites, $v = e^2/a$ is the magnitude of the electrostatic interaction between two charges at distance a , and $w = a/r$. In the following we consider $v = 1$ or 2 , that, for typical $\sqrt{2}t = 1$ eV values,^{22,23} correspond to molecular lengths $a \sim 14$ or 7 Å, respectively. Results will be presented for w increasing from 0 (the gas phase limit) up to a few units (intermolecular distance corresponding to a fraction of the molecular length). For B-lattices $w = 1$ represents an upper bound. For clusters of N molecules the above Hamiltonian is written on the 2^N basis obtained from the direct product of the two basis states located on each molecular site. The eigenstates are obtained by exact diagonalization for systems with up to 16 site, by exploiting translational symmetry.

III. THE MEAN FIELD AND EXCITONIC APPROACHES

In order to better appreciate the physics of interacting polar and polarizable molecules, we will compare exact solutions of the Hamiltonian in Eq. (4) with those obtained within the mf and excitonic approximations. Both approximations are based on the assumption that in the gs the electronic motion on different sites is uncorrelated, so that the gs describes a collection of molecules each one in the local (molecular) gs: $|0\rangle = |G_1 G_2 \dots G_i \dots\rangle$, where $|0\rangle$ represents the mf gs wavefunction for the cluster, and $|G_i\rangle$ is the gs wavefunction for the i -th site. For a cluster of non-overlapping Mulliken molecules the local gs, $|G_i\rangle$, necessarily retains the same form as in Eq. (3), but with ρ depending on the surrounding. In any case, for any given ρ , $|G_i\rangle$ and $|E_i\rangle$ define a couple of local mutually orthogonal wavefunctions, and the 2^N basis functions obtained from the direct product of these local states is a complete basis for the cluster. We define the Pauli matrix operators working on the local $|G_i\rangle$ and $|E_i\rangle$ basis, $\hat{S}_{z/x,i}$, as linear combinations of the Pauli operators, $\hat{\sigma}_{z/x,i}$, working on the original $|DA\rangle$ and $|D^+A^-\rangle$ basis, as follows:

$$\begin{aligned}\hat{S}_{z,i} &= (1-2\rho)\hat{\sigma}_{z,i} + 2\sqrt{\rho(1-\rho)}\hat{\sigma}_{x,i} \\ \hat{S}_{x,i} &= -2\sqrt{\rho(1-\rho)}\hat{\sigma}_{z,i} + (1-2\rho)\hat{\sigma}_{x,i}\end{aligned}\quad (7)$$

To make contact with standard notation¹² we construct the following hard-core boson operators:

$$\begin{aligned}\hat{S}_{x,i} &= (\hat{b}_i^\dagger + \hat{b}_i) \\ \hat{S}_{z,i} &= 1 - 2\hat{b}_i^\dagger\hat{b}_i\end{aligned}\quad (8)$$

These operators have a very clear physical meaning: working on the vacuum state $|0\rangle$, defined as the state where all sites are in the local $|G_i\rangle$ state, \hat{b}_i^\dagger switches the i -th site to the local $|E_i\rangle$ state, and $\hat{n}_i = \hat{b}_i^\dagger\hat{b}_i$ returns the 0 and 1 value for the $|G_i\rangle$ and $|E_i\rangle$ state, respectively. In terms of these operators the Hamiltonian in Eq. (4) reads:

$$H = H_{mf} + H_{ex} + H_{uex} \quad (9)$$

where:

$$\begin{aligned}H_{mf} &= \sum_i \left[2(1-2\rho)(z_0 + M\rho) + 4\sqrt{\rho(1-\rho)} \right] \hat{n}_i \quad (10) \\ &\quad + \sum_i \left[2\sqrt{\rho(1-\rho)}(z_0 + M\rho) - (1-2\rho) \right] (\hat{b}_i^\dagger + \hat{b}_i) \\ H_{ex} &= \sum_{i>j} V_{ij} \left[\rho(1-\rho)(\hat{b}_i^\dagger\hat{b}_j + \hat{b}_j\hat{b}_i^\dagger) + (1-2\rho)^2\hat{n}_i\hat{n}_j \right] \quad (11) \\ H_{uex} &= \sum_{i>j} V_{ij} \left[\rho(1-\rho)(\hat{b}_i\hat{b}_j + \hat{b}_j^\dagger\hat{b}_i^\dagger) \right. \\ &\quad \left. + 2(1-2\rho)\sqrt{\rho(1-\rho)}(\hat{b}_i^\dagger + \hat{b}_i)\hat{n}_j \right] \quad (12)\end{aligned}$$

and $M = \sum_{i>j} V_{ij}/N$.

Three terms in the Hamiltonian in Eq.(9) have been conveniently grouped: the first one, H_{mf} , collects on-site terms, and, as it will be discussed below, sets the basis for the mf description of the gs. Both H_{ex} and H_{uex} work on two sites: H_{ex} conserves the total number of excitations and hence enters the excitonic Hamiltonian, whereas H_{uex} mixes up states differing by one or two excitation, it represents an ultraexcitonic term that will be disregarded in the excitonic approximation.

The transformation in Eq. (7) holds true for any $0 \leq \rho \leq 1$, and the total Hamiltonian in Eq. (9) is not affected by the specific choice of ρ . Of course, its partitioning into the three terms instead varies with ρ , and different excitonic approximation can be derived from the same model Hamiltonian, depending on the specific choice of ρ , or, equivalently, on the specific choice of the local $|G_i\rangle$ and $|E_i\rangle$ wavefunctions. It is important to realize, however, that the second term in H_{mf} does not conserve the exciton number and must be killed in the excitonic approximation. We therefore define the *best* excitonic

Hamiltonian for our model by fixing ρ as to impose the exact vanishing of this term:

$$2\sqrt{\rho(1-\rho)}(z_0 + M\rho) - (1-2\rho) = 0 \quad (13)$$

This equation defines the best local basis for the relevant Hamiltonian in terms of the same $|G_i\rangle$ and $|E_i\rangle$ states defined for the isolated molecule in Eq. (3), but with $z = z_0 + M\rho$ playing the same role as z_0 in the definition of ρ in Eq (13). With this specific choice of ρ the uncorrelated gs $|0\rangle = |G_1 G_2 \dots G_i \dots\rangle$ coincides with the gs of the excitonic Hamiltonian, i.e. of $H_{mf} + H_{ex}$. Since $|0\rangle$ is the gs of an Hamiltonian where all on-site terms are retained, it also represents *the best uncorrelated gs* for the system and indeed coincides with the mf gs. Within mf the cluster is modeled as a collection of non-interacting molecules, each molecules experiencing the electric field generated by the surrounding.^{8,24} This local electric field is responsible for the renormalization of the energy gap between the local I and N states from the value relevant to the isolated molecule ($2z_0$) to $2(z_0 + M\rho)$, relevant to the molecule embedded in a cluster of molecules with average polarity ρ .²⁴

The solution of the two-state problem defined by the local mf Hamiltonian fully defines the excitonic and ultraexcitonic Hamiltonians. Exciting a molecule costs an energy $\hbar\omega_{CT} = 1/\sqrt{\rho(1-\rho)}$, and, with ρ fixed at the mf value, H_{mf} can be rewritten as:

$$H_{mf} = \hbar\omega_{CT} \sum_i n_i \quad (14)$$

This Hamiltonian counts the number of excited molecules in the cluster and assigns energy $\hbar\omega_{CT}$ to each of them. We can also write explicit expressions for the local transition dipole moment, $\mu_{CT} = \mu_0\sqrt{\rho(1-\rho)}$, and for the local mesomeric dipole moment (the difference between the dipole moment in the $|E_i\rangle$ and $|G_i\rangle$), $\Delta\mu = \mu_0(1-2\rho)$. Then, the first term in H_{ex} (Eq. (11)) describes the interactions between transition dipole moments on different molecules: it corresponds to J -type interactions in the standard excitonic model, the only term, beyond H_{mf} in Eq. (14), that survives in the excitonic approximation for apolar molecules.¹² The second term in Eq. (11) accounts for electrostatic interactions between permanent molecular dipole moments: it vanishes for apolar molecules. H_{uex} in Eq. (12) collects ultraexcitonic terms, i.e. terms that mix up states with a different number of excitons. The first term in Eq. (12) has the same origin as the exciton hopping, and is usually referred to as the non Heitler-London term.¹⁴ The second term in the ultraexcitonic Hamiltonian vanishes for apolar molecules.

Of course the Hamiltonian in Eq. (9) exactly maps on the general Hamiltonian derived by Agranovich for a cluster of two-level molecules only interacting via electrostatic forces.¹² However, in the standard excitonic approximation to the general Hamiltonian, the local ground and excited states coincide with the eigenstates of the isolated molecule. Environmental contributions to the

excitation energies (the term proportional to $M\rho$ in the first term of H_{mf}) are accounted for, but any mixing of the two local eigenstates due to environmental effect is neglected (the term proportional to $M\rho$ in the second term in H_{mf} is disregarded).¹² This amounts to a complete neglect of the molecular polarizability: the interaction with the surrounding only affects excitation energies, but not local wavefunctions. Most often the local ground and excited states are defined in terms of effective molecular states as affected by environmental interactions, but the parameters entering the excitonic model are then freely adjustable and can hardly be related to the molecular structure and/or to the supramolecular arrangement. Our choice of the local ground and excited states as the eigenstates of H_{mf} not only defines the best excitonic basis and relates the excitonic and mf pictures, but also leads to an unambiguous definition of the excitonic and ultraexcitonic Hamiltonians. In fact, the mf model relevant to a cluster of non-overlapping molecules is defined, for any specific cluster geometry, given the model Hamiltonian for the isolated molecule.⁸ At variance with the standard implementation of the excitonic model, for either apolar or polar molecules, in our approach all the parameters entering the excitonic (and ultraexcitonic) Hamiltonian, including the excitation energy, the exciton hopping term and the exciton-exciton interaction, are defined by the solution of the (self-consistent) mf local Hamiltonian and can be related to the molecular and supramolecular structure. The solution of the local mf problem is a trivial task for clusters of polar and polarizable molecules described in this paper, where only two states are enough to capture the (low-energy) molecular physics. For MM, like those made up of non-polar molecules, where dispersion forces dominate intermolecular interactions, setting up and solving the local mf problem is a more delicate problem since several molecular states must be explicitly accounted for. In any case, uncovering the relation between the local mf solution of the cluster Hamiltonian and its excitonic (and ultraexcitonic) description is an important result since it allows to set up the description of a MM based on information relevant to the isolated molecule, opening the way to understand the properties of MM from the molecular up to the supramolecular level.

IV. THE GROUND STATE

Figure 2 shows the evolution of the gs polarity vs the inverse intermolecular distance for A, B, and C clusters with $v = 1$ and two different z_0 values. In cluster A repulsive intermolecular interactions disfavor the charge separation on molecular sites and ρ decreases with w . Just the opposite occurs in B and C clusters where attractive interactions favor charge separation. An isolated molecule with an almost neutral gs ($\rho \sim 0.15$ at $w = 0$ for $z_0 = 1$) becomes even more neutral in the repulsive, A-cluster, but, with increasing intermolecular interactions,

it becomes more and more I in attractive (B or C) lattices. For the data in Fig.2, the N chromophore crosses the $\rho = 0.5$ interface separating a N from an I gs at $w \sim 2$ in C-lattice, i.e. at an inter-chromophore separation ~ 5 Å for typical molecular length ~ 10 Å. In B-lattices the interface is located at $w \sim 0.75$, corresponding to intermolecular contacts ~ 3 Å. Conversely, molecules with a zwitterionic gs in the gas phase ($\rho \sim 0.85$ at $w = 0$ for $z_0 = -1$) can be driven to a N gs in the repulsive, A-lattice at $w \sim 1.5$, corresponding to intermolecular distances ~ 7 Å. Even more interesting is the observation that the same molecule in different supramolecular arrangements can have qualitatively different gs, and hence distinctively different properties. Consider e.g. an isolated molecule with an N gs ($z_0 = 1$): in an A-type lattice with $w \sim 3$ (i.e. for intermolecular distances \sim one third of the molecular length) the molecular polarity stays basically unaffected (it slightly decreases down to ~ 0.1). The same molecule in a C-lattice with similar intermolecular distance becomes instead very polar, with $\rho \sim 0.9$ corresponding to an almost zwitterionic gs. Since the properties of push-pull chromophores largely depend of ρ ,²⁵ very different behavior is predicted for different MM made up by the same molecular unit.

Dashed lines in Fig 2 show mf results for the gs polarity: as far as ρ is concerned, the mf approach works well at least for not too large interactions. Within mf we can also understand the qualitatively different behavior of attractive and repulsive lattices. As discussed in the previous Section, within mf ρ is given by Eq. (2), but with $z = z_0 + M\rho$ playing the same role of z_0 , so that:²⁴

$$\frac{\partial \rho}{\partial z_0} = \frac{d\rho}{dz} \left(1 - M \frac{d\rho}{dz} \right)^{-1} \quad (15)$$

$\rho(z)$ has a negative slope, so that for repulsive lattices with $M > 0$, the slope of $\rho(z_0)$ decreases in magnitude with M , justifying the smooth evolution of the $\rho(w)$ curves in Fig.2A. Just the opposite occurs for attractive lattices ($M < 0$). In this case $\partial \rho / \partial z_0$ becomes more negative with increasing the strength of inter-site interactions and, for $M < -2$, it changes its sign, marking the occurrence of a discontinuous phase transition from the N to the I regime. The mf N-I crossover is located at $z = 0$, and S-shaped $\rho(w)$ curves are therefore calculated within mf for systems with $z_0 > 1$, as shown in Fig. 3 for B and C lattices with $v = 2$ and $z_0 = 1.5$ and 2. Regions with negative slope in the mf $\rho(w)$ curves correspond to unstable states, and a bistable regime appears where two stable states ($\partial \rho / \partial w > 0$) coexist for the same w .²⁴ Demonstrating the appearance of a discontinuous interface from exact diagonalization of finite clusters Hamiltonians is hardly possible. In fact only *stable* states are accessible by exact diagonalization: neither the unstable nor metastable states appear in exact curves. In any case, results from exact diagonalization (symbols in Fig. 3) show, at large z_0 , a well pronounced discontinuity, consistent with the discontinuous behavior recognized within mf.

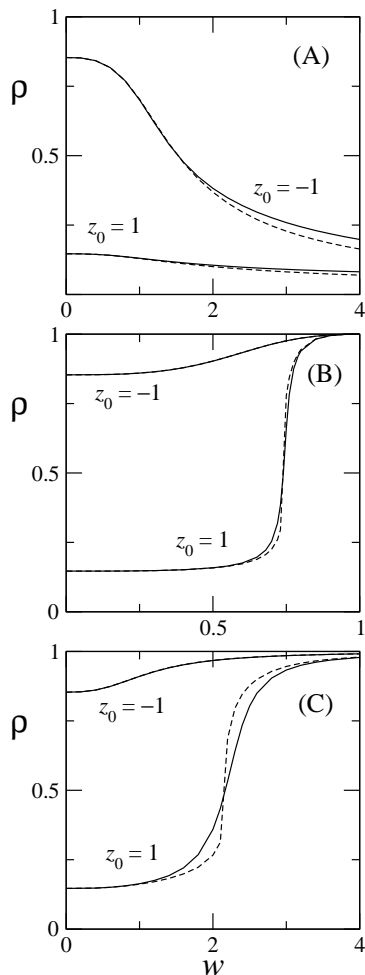


FIG. 2: Ionicity vs the inverse intermolecular distance for A, B and C, lattices with $v=1$ and $z_0 = \pm 1$ Dashed lines: mf results for $N = \infty$; continuous lines: exact results for $N = 16$.

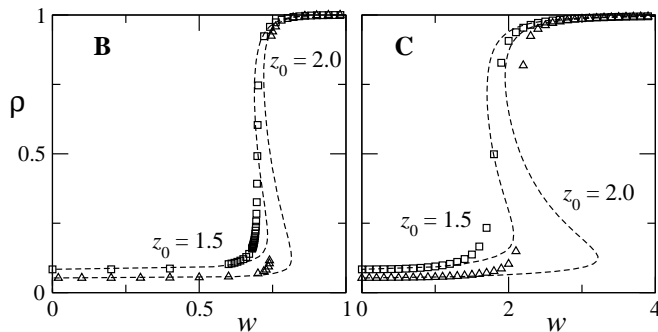


FIG. 3: Exact ionicity vs the inverse intermolecular distance for attractive, B and C, lattices with $N=16$, $v=2$ and $z_0=1.5$ (squares) and 2 (circles). Dashed line show $N = \infty$ mf results.

Isolated (gas phase or solvated) molecules cannot support any kind of phase transitions: the appearance of a discontinuous N to I crossover is one of the most impressive evidences of the cooperative behavior of MM made up of polar and polarizable chromophores. In the proximity of the discontinuous crossover large deviations from the mf picture are expected on general grounds, due to the failure of the non-correlated description of the gs. Correlations effects in this region have important spectroscopic consequences and will be discussed in detail in Sect. VII.

V. THE EXCITATION SPECTRUM

The solution of the local mf problem defines the best local basis $|G_i\rangle$ and $|E_i\rangle$ for the excitonic problem and hence the optimal excitonic approximation for the Hamiltonian in Eq. (4). Figs. 4, 5, and 6, compare the complete set of exact eigenstates (circles) with the excitonic eigenstates (crosses) for A, B, and C clusters, respectively. To avoid overcrowding, data are shown for $N = 6$. In the figures, the excitation energy (i.e. the energy minus the gs energy) is reported for each eigenstate vs $n = \langle \sum_i \hat{n}_i \rangle$, the exciton number. We set $z_0 = -/+1$ for repulsive/attractive lattices (cf Fig. 2). For each cluster we consider two different w values, corresponding to interactions of weak and medium strength (upper and lower panel, respectively). For reference purposes, the inset in each panel shows the mf $\rho(w)$ curve, with the vertical dotted line marking the relevant w values.

Within the excitonic approximation n is conserved: excitonic eigenstates line up exactly in Figs. 4, 5, and 6, defining bands of states with integer n . The excitonic bandwidth measures the amount of mixing of states with the same n , induced by the exciton hopping (the first term in Eq. (11), corresponding to J -like interactions in the standard excitonic model) and by the exciton-exciton interaction term (the second term in Eq. (11), relevant to polar molecules). This last term affects the energy of multi-exciton states lowering (increasing) the energy of states with several nearby excitations in attractive (repulsive) lattices.

The ultraexcitonic Hamiltonian in Eq. (12) mixes up states with different n . For weak interactions (upper panels in Fig. 4, 5, and 6) the ultraexcitonic mixing is not large, and n is approximately conserved also for the exact eigenstates (circles). But, for larger interactions (bottom panels), the combined role of exciton-exciton interactions and of the ultraexcitonic mixing can have important consequences.

Figs. 4, 5, and 6 carry one more information: The size of the error-bars attached to each symbol are proportional to the transition dipole moment from the gs toward the relevant eigenstate. A general selection rule applies to both exact and excitonic eigenstates: only zero wavevector ($k = 0$) states are reached by optical transition. Moreover, within the excitonic approximation, only

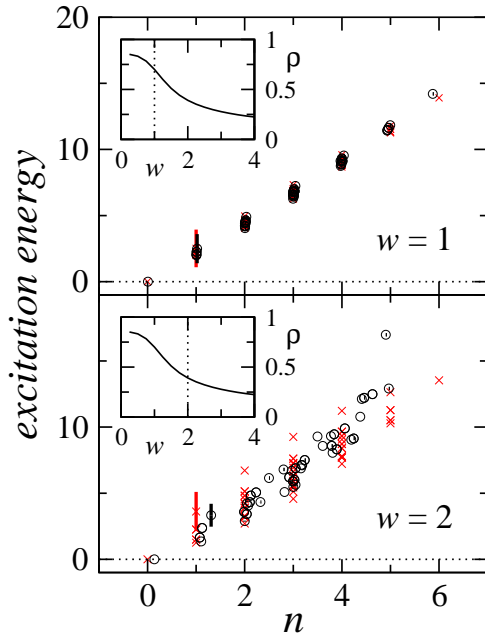


FIG. 4: Excitation spectrum of an A-lattice with $N = 6$, $v=1$, $z_0 = -1$ and two different w . Circles and crosses show the excitation energy for exact and mf eigenstates, respectively, against the number of excitons. States on the zero energy axis correspond to the gs. Error bars measure the squared transition dipole moment from the gs to the relevant states. Insets show the $\rho(w)$ mf curve for the relevant parameters, with the dotted vertical line marking the w value for which results are reported in the parent panel.

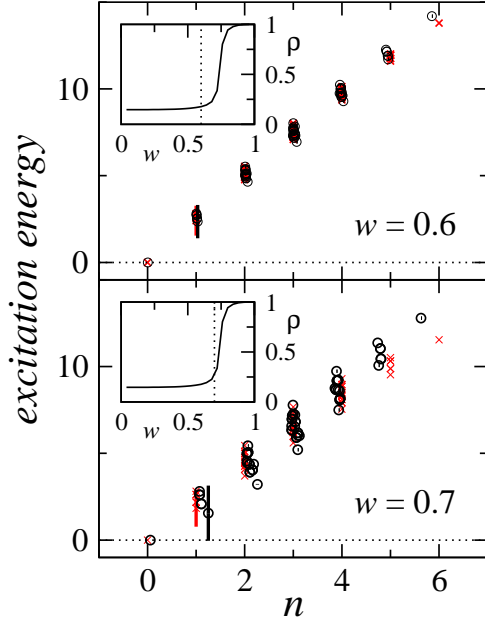


FIG. 5: The same as in Fig. 4, but for B-lattices with $v = 1$, $z_0=1$ and two different w .

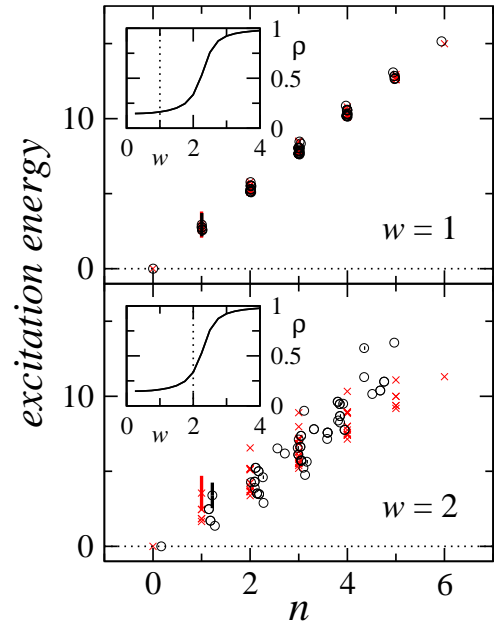


FIG. 6: The same as in Fig. 4, but for C-lattices with $v = 1$, $z_0=1$ and two different w .

one excitation can be created upon one-photon absorption so that only the state with $k = 0$ and $n = 1$ has a finite transition dipole moment from the gs. This state is at the top of the $n = 1$ exciton band in the repulsive A lattice ($J > 0$, H-aggregates) and at the bottom of the one-exciton band in the attractive, B-lattice ($J < 0$, J-aggregate). C-lattice with two molecules per unit cell is different: the inversion symmetry that relates the two molecules in the unit cell allows to classify the two $k = 0$ one-exciton states as symmetric and antisymmetric, and only the antisymmetric state is optically active. This state corresponds to a $k = \pi$ state in the extended zone representation, and for this *attractive* lattice ($J < 0$) the optically allowed state actually lies at the top of the one-exciton band.

The ultraexcitonic mixing relaxes the $\Delta n = 1$ selection rule of the excitonic model and the oscillator strength can spread over several $k = 0$ states. However, at least for the cases shown in Figs. 4, 5, and 6, a single excited state retains most of the oscillator strength, leading to a spectral behavior qualitatively similar as in the excitonic picture. However, for not too weak interactions (bottom panels in Figs. 4, 5, and 6) the exciton number in the most optically allowed state distinctively deviates from the excitonic result ($n = 1$). More generally, the excitonic description of the photoexcited state is not very accurate. Consider, just as an example, a B-lattice with parameters as in Fig. 5, upper panel. As for the data reported in the figure are concerned, the excitonic picture works fairly well. However, the average ionicity of the optically allowed state calculated in the excitonic picture is about $\sim 15\%$ smaller than the exact result. The differ-

ence becomes $\sim 40\%$ for the parameters in the bottom panel of the same figure. The discrepancy between excitonic and exact descriptions of the states reached upon photoexcitation becomes more and more evident as the discontinuous charge crossover is approached, and will be discussed in greater detail in Sect. VII.

VI. STATIC SUSCEPTIBILITIES

Collective effects that are discussed in the previous Section with reference to excitation spectra, must also show up in linear and non-linear susceptibilities of MM. Here we focus attention on the linear susceptibility α and on the first hyperpolarizability β , defined by the expansion of the gs polarization, P (the dipole moment per unit volume) vs a static electric field, F , as follows:

$$P(F) = P(0) + \alpha F + \frac{1}{2}\beta F^2 + \dots \quad (16)$$

Continuous lines in Fig. 7 report exact α and β values calculated as a function of w for 16-site clusters with $v = 1$. Top panels refer to an A-cluster with $z_0 = -1$, middle and bottom panels refer to B and C clusters, respectively, with $z_0 = 1$. The cluster susceptibilities deviate considerably from those relevant to the isolated molecules, and a large and non-trivial dependence of the optical responses on the supramolecular arrangement is observed. This is due to the large response of polarizable molecules to the local electric fields in the material, and has important, and so far not fully appreciated, consequences.

Some degree of non-additivity of the optical responses of clusters of push-pull chromophores could have been guessed from the large dependence of the gs molecular polarity on supramolecular interactions, as shown in Fig. 2 and 3. For push-pull chromophores in fact linear and non-linear optical responses strongly depend on ρ . Since closed expressions for α and β as a function of ρ are available,²⁵ the simplest approach to static susceptibilities relies on a *mf oriented gas* picture. Within mf the gs of the cluster describes a collection of non-interacting molecules. The responses of a cluster of molecules can accordingly be calculated as the sum of contributions from the molecules in the relevant mf gs. The susceptibilities obtained in this approximation (dotted lines in Fig. 6) deviates considerably from exact results, a particularly impressive result in view of the reliability of mf estimates of ρ for the same clusters (cf Fig. 2). The oriented gas approach to susceptibilities fails since the response of a molecule to an applied field strongly depends on the molecular environment.

As a matter of fact, the mf approximation leads to fairly accurate estimates of the susceptibilities for MM, provided the oriented-gas approximation is relaxed. Dashed lines in Fig. 7 show the susceptibilities calculated as successive F -derivatives of the polarization of

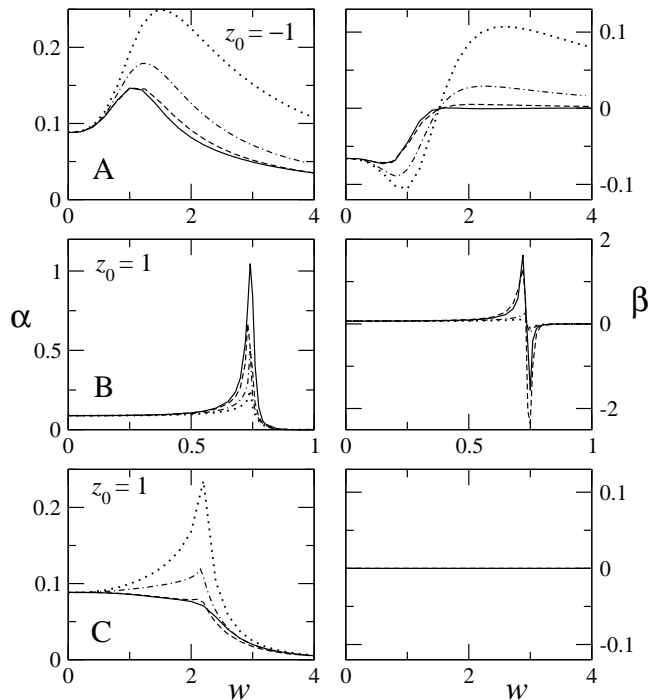


FIG. 7: Linear susceptibility (α) and first hyperpolarizability (β) vs the inverse intermolecular distance for A, B and C clusters (upper, middle and lower panels, respectively) with $N = 16$, $v=1$ and $z_0 = \pm 1$. Dotted lines: mf-oriented gas approximation; dot-dashed line: excitonic approximation; dashed lines: mf approximation; continuous lines: exact results. The β response for C-clusters vanishes by symmetry.

the cluster, calculated in the mf approximation. Apart from small deviations that appear just in the crossover regime where the mf estimate of ρ is slightly inaccurate by itself (cf Fig. 3), the mf susceptibilities nicely agree with exact results. The large deviations between the susceptibilities calculated as sum of molecular mf contributions (mf oriented gas approximation, dotted lines in Fig. 7) and those obtained from the successive derivatives of the mf polarization of the cluster (mf results, dashed lines in Fig. 7) are a direct measure of collective effects, and can be understood since the polarization of the cluster is the sum of the (oriented) dipole moments calculated for each molecule, but its derivatives with respect an applied field largely deviate from the sum of the corresponding derivatives (as imposed in the oriented gas model).

Sum over state (SOS) expressions directly link static susceptibilities to the excitation spectrum,²⁶ offering a way to estimate the magnitude of excitonic and ultraexcitonic contributions to static optical responses. For sure susceptibilities evaluated from the successive derivatives of the gs polarization and from SOS expressions do coincide, provided they are obtained from the eigenstate of the same Hamiltonian.²⁷ Then exact SOS susceptibilities coincide with the F derivatives of the exact gs polarization. Similarly, the susceptibilities obtained in the mf

oriented gas approach, coincide with the SOS susceptibilities calculated for a collection of non-interacting (mf) molecules. The large deviations of the mf-oriented gas susceptibilities from exact results can then be ascribed to the combined effect of excitonic and ultraexcitonic mixing in the excitation spectrum. The complete diagonalization of the excitonic Hamiltonian ($H_{mf} + H_{ex}$) and the subsequent calculation of SOS susceptibilities leads to results reported as dot-dashed lines in Fig. 7. Accounting for excitonic interactions considerably improves over the oriented gas estimate of static susceptibilities. However, sizeable deviations from exact results are observed, pointing to the importance of ultra-excitonic effects. In particular we underline that large ultraexcitonic contributions to both α and β are observed even in regions where the mf approximation gives a fairly accurate description of both the gs polarity and of the static susceptibilities. Neglecting the molecular polarizability in the description of excited states, as imposed in the excitonic approach, is a dangerous approximation for linear and non-linear optical responses of molecular materials made up of polar and polarizable molecules.

VII. COLLECTIVE AND COOPERATIVE EFFECTS AT THE DISCONTINUOUS CHARGE CROSSOVER

As discussed in Sect. III, the mf approximation applied to attractive lattices with $z_0 > 1$ leads to S-shaped $\rho(w)$ curves (cf Fig 3), that signal the occurrence of a discontinuous phase transition. The excitation spectrum of the system near the discontinuous charge crossover is interesting and deserves detailed discussion. Figs. 8 and 9 show the excitation spectrum calculated for B and C clusters in the N regime, but very near to the discontinuous crossover. Results are shown for clusters of 10 sites and, for the sake of clarity, only zero wavevector eigenstates are reported, with circles and crosses referring to exact and excitonic results, respectively.

Near the discontinuous crossover the excitation energy ($\hbar\omega_{CT}$ in Eq. (14)) is at a minimum and exciton hopping and exciton-exciton interactions are large enough to induce a partial overlap of excitonic bands (cf crosses in Figs 8, 9). Ultraexcitonic mixing is therefore very effective: the exciton number is not even approximately conserved in exact eigenstates. Moreover, the energy of exact excited states show a non-monotonic dependence on the exciton number. In particular, in B and C lattices the lowest excited state corresponds to a state with more than 3 and 2 excitons, respectively. This result contrasts sharply with the excitonic picture, where the excitation energy increases monotonously with the exciton number, so that the lowest excitation energy corresponds to the creation of a single exciton.

As a matter of fact, the excitonic picture is completely spoiled in the bistability region. Whereas this is not particularly surprising, it is important to realize that many

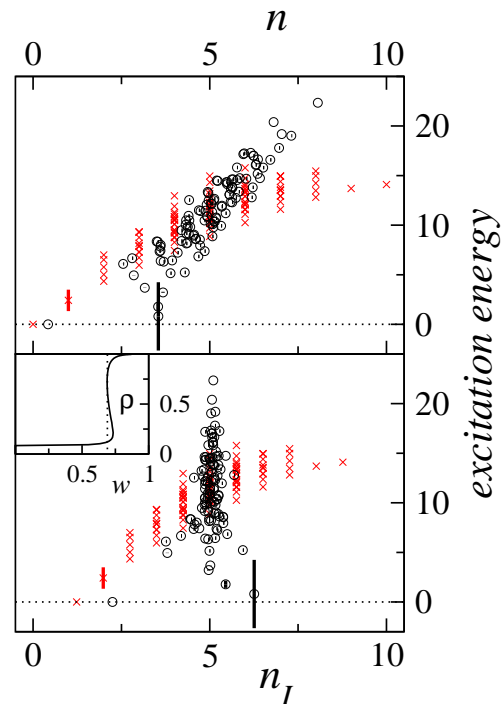


FIG. 8: Excitation energies for the zero wavevector eigenstates of a 10-site B-cluster with $v = 2$, $z_0 = 1.5$ and $w = 0.69$ reported against the number of excitons (upper panels) and the number of I molecules (bottom panels). Circles and crosses refer to exact and excitonic eigenstates, respectively. States on the zero energy axis correspond to the gs. Error bars measure the squared transition dipole moment from the gs to the relevant states. The inset shows the corresponding $\rho(w)$ mf curve, with the vertical dotted line marking the relevant w value.

concepts usually adopted to discuss excitations in molecular crystals fail there. In particular, the very same concept of excitation is challenged by exact results for B and C clusters near the discontinuous crossover. Both lattices in fact have in the gs a number of excitons distinctively larger than zero (cf Figs.8 and 9 where the exact gs eigenstate has $n > 0$). In these conditions the definition of a local excitation is somewhat artificial. We therefore go back to the original $|DA\rangle$ and $|D^+A^-\rangle$ basis and, in the lower panels in Figs.8 and 9 we report the same excitation spectrum as in the upper panels, but with the abscissa axis now measuring the average number of fully-I ($|D^+A^-\rangle$) sites, i.e. the expectation value of $\hat{n}_I = \sum_i \hat{\rho}_i$. The operator \hat{n}_I is diagonal on the excitonic eigenstates: in the excitonic approximation n_I and n are related by a simple expression, $n_I = N\rho + (1 - 2\rho)n$, where n_I , and n are the expectation values of the corresponding operators in the given state and ρ is the mf molecular ionicity. Excitonic eigenstates then line up vertically also when reported against n_I (cf crosses in Figs. 8 and 9). For exact eigenstates instead n and n_I carry independent information.

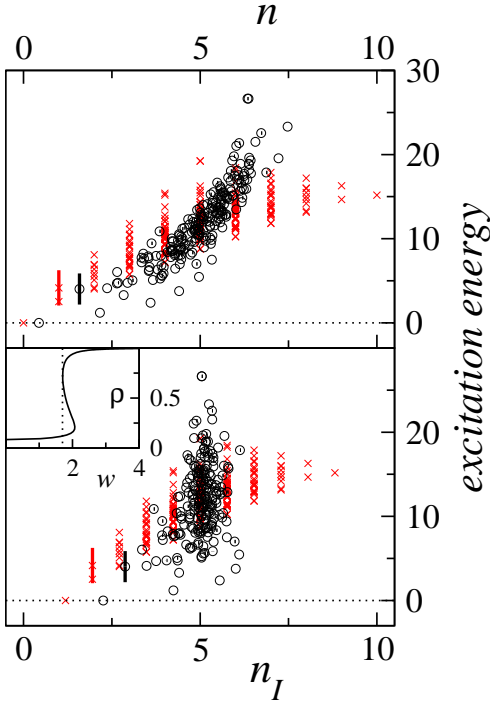


FIG. 9: The same as in Fig. 8 for a C cluster with $v = 2$, $z_0 = 1.5$ and $w = 1.7$. For graphical purposes the error bars measuring the transition dipole moments have been magnified by a factor of two with respect to those reported in Fig. 8.

In any case, n_I is finite in both the exact and excitonic gs to indicate a finite ρ . The difference between the excitonic and exact n_I of course parallels the sizeable difference between the mf and exact ρ observed near the discontinuous crossover (cf Fig. 3). More interesting is the behavior of the lowest excited state: in both B and C lattices the lowest excitation corresponds to a state whose n_I appreciably differs from the gs value: the lowest exact excited states has a very different nature from the gs. This contrasts with the excitonic picture where the lowest excited state is a state with a single excitation, whose ionicity differs from the gs ionicity by $|1 - 2\rho| \leq 1$.

Attractive supramolecular interactions in B and C lattices lead to a qualitatively similar $\rho(w)$ dependence (cf Figs. 2, 3). The two lattices however have different symmetry and hence a *qualitatively* different spectroscopic behavior, as already discussed in Sec. V. Lattice B has one molecule per unit cell and all $k = 0$ states are optically allowed, even if most of them have negligible intensity. The two molecules per cell in lattice C are exchanged by reflection, so that only $k = 0$ antisymmetric states are accessible by one-photon absorption from the (totally-symmetric) gs: about half of the exact $k = 0$ states in Fig. 9 are actually dark states. The special low-energy state with large n is a dark state in C-clusters, but corresponds to the state with the largest oscillator strength in B-clusters (cf Fig. 8, and 9). The spectroscopic behavior of B-lattices is therefore particularly interesting and will

be discussed in greater detail below.

Data in Fig. 8 show that upon absorption of a single photon about 3 excitons are created in B-lattice, or ~ 4 molecules are switched from N to I. This implies of course that the motion of ~ 4 electrons is driven by the absorption of a single photon. In B-lattices near the discontinuous interface the primary photoexcitation event therefore corresponds to a *multielectron transfer*.²⁸ This sharply contrasts with the excitonic picture where a single molecule is excited by a single photon, leading to the transfer of no more than a single electron (specifically $|1 - 2\rho| \leq 1$ electrons are transferred upon photoexcitation). Multielectron transfer is a new phenomenon with no counterpart in the standard description of optical excitations in MM. The theoretical and practical implications of multielectron transfer are hardly overemphasized.²⁹ Here we underline that so far multielectron transfer was discussed as a secondary photoexcitation event: the absorption of a photon induces a single electron transfer, then cooperative interaction with slow degrees of freedom (either vibrational or environmental) leads to multiple electron transfer via a cascading effect.²⁹ In our model direct (vertical) photoexcitation of several electrons is made possible by the correlation of electronic motion on different (non-overlapping) molecules for systems at the discontinuous charge crossover.²⁸

Data in Fig. 8 refer to a 10 site cluster, but multielectron transfer safely survives in longer chains. With reference to the excited state with the largest transition dipole moment, we calculate both the excitation energy and the average number of molecular sites turned I upon excitation (ν_I , defined as the difference between n_I in the excited and ground state). Left panels in Fig. 10 show the N-dependence of these two quantities calculated for a B-lattice with $v = 2$, $z_0 = 1.5$, and several w . For w increasing from 0.60 to 0.69 the system is driven towards the interface (cf Fig. 3) and ν_I smoothly extrapolates to $N \rightarrow \infty$, with values that increase from ~ 1.2 ($w = 0.60$) to 2.5 ($w = 0.68$). Finite-size effects are larger at $w = 0.69$, but ν_I clearly extrapolates to even larger (~ 3) values there. The corresponding excitation energy smoothly extrapolates towards finite values in the $N \rightarrow \infty$ limit (Fig. 10, upper panel): in an infinite linear chain with B-geometry, near the discontinuous charge crossover the absorption of a single optical photon (with energies ~ 1 eV for the parameters in Fig. 10 and $\sqrt{2}t = 1$ eV) drives the coherent motion of several (~ 3) electrons.

The right panels in Fig. 10 show the behavior of a B-lattice near to a discontinuous charge crossover with a much larger ionicity jump with respect to case shown in the left panel (cf. Fig. 3). Results are even more impressive there: depending on the model parameters, in fact up to 8 electrons can be transferred by absorption of a single photon. However, the finite-size analysis requires in this case much longer chains than addressed here (at least a few times longer than the number of electrons transferred).

To better understand the physics of multielectron

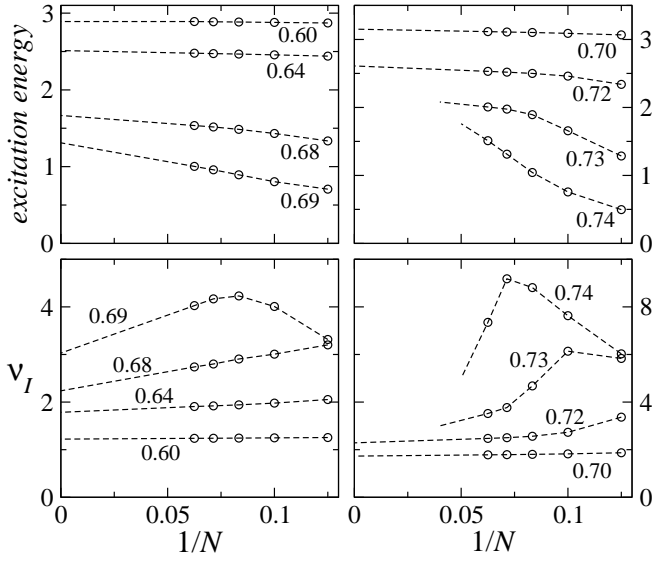


FIG. 10: The $1/N$ dependence of the excitation energy and of the average number of molecules turned I upon photoexcitation. Results refer to the state with the largest transition dipole moment for B-clusters with $v = 2$, and $z_0 = 1.5$, and 2 (left and right panels, respectively). The numbers labelling each curve show the corresponding w value. Lines are drawn as guide for eyes.

transfer we define the following l -th order correlation function:

$$f_l = \sum_{i=1}^N \langle \hat{\rho}_i \hat{\rho}_{i+1} \dots \hat{\rho}_{i+l-1} \rangle - \sum_{i=1}^N \langle \hat{\rho}_i \rangle^l \quad (17)$$

f_l vanishes exactly for uncorrelated states, that is for states that can be reduced to the product of local molecular states. Positive (negative) f_l indicates an increased (decreased) probability of finding l nearby I molecules with respect to the uncorrelated state with the same average polarity. The upper panel of Fig. 11 shows the l -dependence of f_l calculated for the most optically active state of a B-cluster with the same parameters as in Fig. 10, just at the N-I crossover ($w = 0.69$). In this state a non-negligible weight is found of wavefunctions with several (2-4) nearby fully-I molecules. Then the photo-induced multielectron transfer corresponds to a *concerted electronic motion occurring on several nearby molecules*.

The bottom panel in Fig. 11 shows the correlation function calculated for the gs: quite predictably the overall degree of correlation is smaller in the ground than in the excited state (notice the different scale on the y-axis in the two panels in Fig. 11). In any case data in Fig. 11 demonstrate a finite contribution to the gs of I-droplet states, i.e. of states with two or more nearby I-sites. Near the discontinuous charge crossover the mf description of the gs fails: the exact gs is not the vacuum state (cf the finite n_e relevant to the exact gs in Fig. 8)

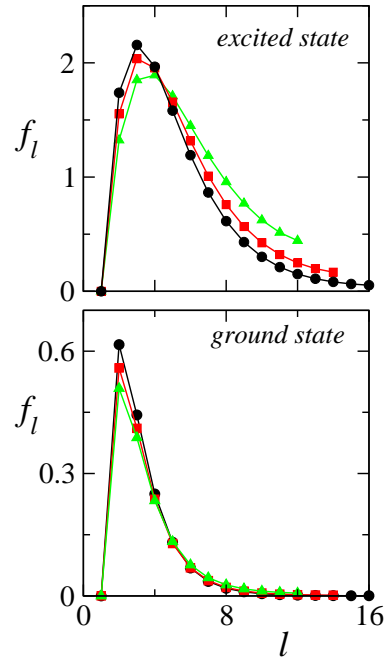


FIG. 11: The l dependence of f_l correlation function calculated for the ground state and for the excited state with the largest transition dipole moment for a B-lattice with $v = 2$, $z_0 = 1.5$ and $w = 0.69$. Triangles, squares and circles shows results for $N = 12, 14$, and 16 , respectively.

and cannot be described as the direct product of local molecular states (cf the finite f_l in the lowest panel in fig. 11). Within the proposed model for *non-overlapping* molecules *classical* electrostatic interactions lead, near the discontinuous crossover, to an intrinsically *collective and correlated* zero-temperature gs. The finite amplitude of I-droplet states in this gs is the key to understand multielectron transfer: in B-clusters, I droplet states have a finite (and large) permanent dipole moment: their finite amplitude in the gs is therefore responsible for the appearance of sizeable transition dipole moments from the gs towards states with a large I-droplet character. This observation also sheds light on the qualitatively different behavior of C and B lattices. For sure the discontinuous crossover in C-lattices is similar in nature to that observed in B-lattices and correlated ground and excited states are expected for these lattices too. However C-lattices are centrosymmetric: droplet states do not have permanent dipole moments and do not contribute to the transition dipole moments.

The behavior of systems lying near the discontinuous crossover, but on the I side is similar to that of N systems, described above, provided the role of $|DA\rangle$ and $|D^+A^- \rangle$ is interchanged. Similar behavior as described in Figs. 10, and 11 can be obtained in fact if ν_I , the number of sites turned I upon photoexcitation is substituted by ν_N , the number of sites turned N. Similarly $1 - \hat{\rho}_i$ must substitute $\hat{\rho}_i$ to define a correlation function measuring

the probability, in each relevant state, of droplets of l nearby N-molecules.

VIII. DISCUSSION

In this paper we have presented a simple and interesting model for clusters of polar and polarizable molecules. Each molecular site is described in terms of a two-state model. Only classical electrostatic intermolecular interactions are accounted for, neglecting any intermolecular overlap of wavefunctions on different molecules. The model applies quite naturally to MM (crystals, aggregates, films..) based on push-pull chromophores, an interesting class of molecules quite extensively investigated for NLO applications.

Push-pull chromophores are largely polar and polarizable molecules, and electrostatic interactions can only be understood within models that properly account for the molecular polarizability at all orders: each molecule in fact experiences in the material the local electric fields generated by the surrounding molecules in a non-trivial feed-back mechanism that is responsible for large collective and cooperative effects. The Mulliken model, adopted for the molecular sites, is particularly interesting in this respect since it accounts for the molecular polarizability and hyperpolarizabilities,²⁵ in a two-state approach that represents the simplest picture to describe polar molecules.

Our model of course maps exactly onto the Hamiltonian derived several years ago by Agranovich for a molecular crystal described as a collection of two-state molecules interacting via electrostatic forces.¹² Being interested in the very weak interaction limit, Agranovich defined the excitonic Hamiltonian by disregarding all terms in the complete Hamiltonian not conserving the exciton number.¹² For polarizable molecules we propose a different strategy: via a rotation of the local (on-site) basis we retain the local term not conserving n . In other words we recognize that the optimal local basis for the excitonic problem coincides with the eigenstates of the local self-consistent mf problem. The relation between the mf and the excitonic approach is fairly fundamental. In the excitonic model excitations are created on top of an uncorrelated gs: the mf solution then gives the best gs for the excitonic problem. The definition of the local states for the excitonic problem as the eigenstates of the local mf Hamiltonian unambiguously defines the excitonic and ultraexcitonic Hamiltonian for any supramolecular arrangement, based on the adopted model for the isolated molecule. Uncovering a direct link from the molecular to the supramolecular description gives an important contribution to our understanding of MM, and is a fundamental step to devise approaches to guide the chemical synthesis of functional MM from the molecular to the supramolecular level.

The mf description of MM can be set up for different kinds of molecules described at different level

of sophistication.⁸ So our approach is widely applicable. Here we have discussed its application to a simple model for clusters of polar and polarizable chromophores where particularly important collective and cooperative effects are expected. Collective effects show up in the gs with the large dependence of the molecular polarity on supramolecular interactions. The effect of the surrounding medium, and specifically of the solvent, in tuning the polarity of push-pull chromophores has already been underlined,^{30,31} and is a natural consequence of the large molecular polarizability. Here we extend this concept to supramolecular interactions in MM and demonstrate that they can widely tune the molecular polarity, and eventually drive it across the N-I interface. The major difference with respect to solvated molecules is the possibility for MM to support true phase transitions, as the extreme manifestation of cooperative behavior.

The properties of isolated push-pull chromophores, and most interestingly, their NLO responses strongly depend on the molecular polarity:²⁵ the large variation of ρ induced by supramolecular interactions then immediately suggests that NLO responses are strongly affected by supramolecular interactions. Apart from a narrow region around the crossover regime, the mf approach nicely approximate the NLO responses of the material. Huge collective effects are demonstrated that are only partly accounted for within the excitonic approximation. The large ultraexcitonic corrections in Fig. 7 suggest that the excitonic model does not provide a reliable approximation scheme for the calculation of NLO responses of MM based on largely polarizable molecules.

The traditional strategy to get molecular materials with large β responses relies on the optimization of β at the molecular level, in the tacit assumption that materials based on molecules with the largest β will have the largest responses. But, in agreement with experimental observation,^{32,33,34} results in Fig. 7 demonstrate that the properties of MM based on push-pull chromophores are far from additive. To guide the synthesis of optimized materials, structure properties relationships must be devised and fully understood not only at the molecular level but also at the supramolecular level. The detailed analysis of the simple model for supramolecular clusters presented here is a first step in this direction.

Deviations of the excitation spectrum from the excitonic description are predictably sizeable for materials with medium-large supramolecular interactions, with more important effects for materials located near the N-I interface where the molecular polarizability is at a maximum. More interesting is the observation of new phenomena driven by cooperativity near the discontinuous charge-crossover of attractive lattices. The lowest excitation of a N (I) lattice near the N-I discontinuous crossover creates an droplet of I (N) molecules whose size increases as the system is driven towards more discontinuous interfaces. These droplet states, that appear as low-lying excitations near the discontinuous N-I crossover, share the same physics with the charge-density-wave droplets ob-

served in half-filled extended Hubbard 1D chains at the discontinuous phase transition from the Mott-insulator to the charge-density wave state,³⁵ and are due to the nucleation of I (N) domains in the presence of large intersite interactions. The main novelty of our result in this respect is the observation that these droplet states are, in a non-centrosymmetric environment, optically allowed, so that the absorption of a single photon in a N (I) material can directly create an I (N) droplet extending over several molecules. The primary photoexcitation event is in these conditions a multielectron transfer that is a direct consequence of the correlation of the electronic motion among different non-overlapping molecules.

We have discussed the gs and the excitation spectrum of a model for polar and polarizable molecular units, only interacting via electrostatic forces. The model naturally applies to MM based on push-pull chromophores, but also offers a rough description of organic CT salts with a mixed stack motif. In these materials, π -conjugated molecules with a strong electron D and A character alternate in a one-dimensional stack: the sizeable overlap between adjacent molecules leads to charge-resonance and hence to fractional charges on molecular sites. The N-I phase transition observed in these materials³⁶ is a fascinating phenomenon whose physics is actively investigated.³⁷ In the early days of the N-I transition, it was modeled by reducing the stack of overlapping molecules into a collection of non-overlapping DA pairs,²⁴ i.e. by adopting exactly the same model proposed here for B-lattice. Of course this approximation is very rough and more refined models are needed to understand the complex and variegated behavior of

CT salts with a mixed stack motif.³⁸ However, the N to I crossover discussed here for attractive lattices of polar and polarizable molecules shares the same physics as the N-I transition in CT salts. In this respect we underline that anomalous spectral features for CT salts in the region of the discontinuous N-I transition were already discussed in Ref.39. In particular the importance of I/N droplet states as well as the failure of the excitonic approximation in the proximity of the discontinuous crossover were addressed. Multielectron transfer, described here for molecular clusters, indeed offers suggestive hints on the physics of photoinduced N-I phase transitions in CT salts.²⁸ However CT salts are extended systems, with electrons delocalized all along the stack. On the opposite, the molecular clusters described here are fully localized systems: electrons cannot escape from their parent molecule. In this respect we underline that the main novelty and interest of the present work is in the observation of cooperative phenomena and correlation effects among *non-overlapping* molecular units.

Acknowledgments

A.P. thanks Z.G.Soos for several enlightening discussions, and S.Mazumdar, S.Ramasesha and F.Spano for useful conversations. F.T. thanks J.Knoester and V.Chernyak for interesting discussions. Work partly supported by the Italian Ministry of Education (MIUR) through COFIN-2001, and by INSTM through PRISMA-2002.

-
- * Electronic address: anna.painelli@unipr.it
- ¹ S.R.Marder, et al., Nature 388 (1997) 8445.
 - ² M.Albota, et al., Science 281 (1998) 1653.
 - ³ M.Blanchard-Desce, et al. Chem.Eur.J. 3 (1997) 1091.
 - ⁴ A.Abbotto, et al. Adv.Mater. 12 (2000) 1963.
 - ⁵ Science 295 (2002), special issue on *Supramolecular chemistry and self-assembly*.
 - ⁶ J.I.Krugler, C.G.Montgomery, H.M.McConnell, J.Chem.Phys. **41**, 2421 (1964).
 - ⁷ C. W. Dirk, R. J. Twieg, and G. Wagnière, J. Am. Chem. Soc. **108**, 5387 (1986).
 - ⁸ E.V. Tsiper and Z.G. Soos, Phys. Rev. B **64**, 195124 (2001)
 - ⁹ Z.G. Soos, E.V. Tsiper and R.A. Pascal, Jr., Chem. Phys. Lett. **342**, 652 (2001)
 - ¹⁰ E.V. Tsiper and Z.G. Soos, Phys. Rev. B (in press).
 - ¹¹ A.S. Davidov, *Theory of molecular excitons* Plenum Press, New York (1971).
 - ¹² V.M.Agranovich, M.D.Galanin, *Electronic excitation energy transfer in condensed matter*, North-Holland, Amsterdam (1982).
 - ¹³ J. Knoester, in *Organic nanostructures: science and applications*, IOS Press, Amsterdam (2002)
 - ¹⁴ L.D.Bakalis, J.Knoester, J. Chem. Phys. **106**, 6964 (1997).
 - ¹⁵ F. C. Spano, V. Agranovich, S. Mukamel, J. Chem. Phys. **95**, 1400 (1991).
 - ¹⁶ F.C.Spano, E.S.Manas, J.Chem.Phys. **103** 5939 (1995).
 - ¹⁷ H. Ezaki, T. Tokihiro, E. Hanamura, Phys. Rev. B **50**, 10506 (1994)
 - ¹⁸ M. Kuwata-Gonokami, N. Peyghambarian, K. Meissner, B. Fluegel, Y. Sato, K. Ema, R. Shimano, S. Mazumdar, F. Guo, T. Tokihiro, H. Ezaki, E. Hanamura, Nature **367**, 47 (1994).
 - ¹⁹ S. Mazumdar, F. Guo, K. Meissner, B. Fluegel, N. Peyghambarian, M. Kuwata-Gonokami, Y. Sato, K. Ema, R. Shimano, T. Tokihiro, H. Ezaki, E. Hanamura, J. Chem. Phys. **104** 9283 (1996); *ibid.* **104** 9292 (1996).
 - ²⁰ R. S. Mulliken, J. Am. Chem. Soc. **74**, 811 (1952).
 - ²¹ J. L. Oudar and D. S. Chemla, J. Chem. Phys. **66**, 2664 (1997)
 - ²² A. Painelli and F. Terenziani, J. Phys. Chem. A **104**, 11041 (2000); F. Terenziani, A. Painelli, and D. Comoretto, *ibid.* **104**, 11049 (2000).
 - ²³ B.Boldrini, E.Cavalli, A.Painelli, and F.Terenziani, J. Phys. Chem. A **106**, 6286 (2002).
 - ²⁴ Z.G.Soos, H.J. Keller, W. Moroni and D. Nothe, Ann.N.Y.Acad.Sci., **313**, 442 (1978).
 - ²⁵ A.Painelli, Chem.Phys.Lett. **285**, 352 (1998), and references therein.

- ²⁶ B.J.Orr, and J.F.Ward, *Mol.Phys.* **20**, 513 (1971).
- ²⁷ L.Del Freo, F.Terenziani, and A.Painelli, *J.Chem.Phys.* **116**, 755 (2002).
- ²⁸ A. Painelli, F. Terenziani, *J. Amer. Chem. Soc.* **125**, 5624 (2003).
- ²⁹ H. Tributsch, L.Pohlmann, *Science*, **279**, 1891 (1998).
- ³⁰ C.Reichardt, *Chem.Rev.*, **94**, 2319 (1994).
- ³¹ A.Painelli, *Chem.Phys.* **245**, 185 (1999).
- ³² M.A.Carpenter, C.S.Willand, T.L.Penner, D.J.Williams, S.Mukamel, *J.Phys.Chem.* **96**, 2801 (1992).
- ³³ A.W.Harper, S.Sun, L.R.Dalton, S.M.Garner, A.Chen, S.Kalluri, W.H.Steier, B.H.Robinson, *J.Opt.Soc.Am.B* **15**, 329 (1998).
- ³⁴ E. D. Rekaï, J.-B. Baudin, L. Jullien, I. Ledoux, J. Zyss, M. Blanchard-Desce, *Chem. Eur. J.* **7**, 4395 (2001).
- ³⁵ E. Jeckelmann, *Phys. Rev. Lett.*, **89**, 236401 (2002)
- ³⁶ J.B.Torrance, J. E. Vazquez, J. J. Mayerle, and V. Y. Lee, *Phys.Rev.Lett.* **46**, 253 (1981); J.B.Torrance, A. Girlando, J. J. Mayerle, J. I. Crowley, V. Y. Lee, P. Batail, and S. J. LaPlaca **47**, 1747 (1981).
- ³⁷ S.Horiuchi, Y. Okimoto, R. Kumai, and Y. Tokura *Science* **299**, 229-232 (2003).
- ³⁸ Y.Anusooya-Pati, Z.G.Soos, A.Painelli, *Phys.Rev.B* **63**, 205118 (2001), and references therein.
- ³⁹ Z.G.Soos, S.Kuwajima, and R.H.Harding, *J.Chem.Phys.* **85**, 601 (1986).